

Descriptors for thermal expansion in solids

Joseph T. Schick,^{1,*} Abhijith M. Gopakumar,² and Andrew M. Rappe²

¹*Department of Physics, Villanova University, Villanova, PA 19085-1478, USA*

²*Department of Chemistry, University of Pennsylvania, Philadelphia, PA 19104-6323, USA*

Thermal expansion in materials can be accurately modeled with careful anharmonic phonon calculations within density functional theory. However, because of interest in controlling thermal expansion and the time consumed evaluating thermal expansion properties of candidate materials, either theoretically or experimentally, an approach to rapidly identifying materials with desirable thermal expansion properties would be of great utility. When the ionic bonding is important in a material, we show that the fraction of crystal volume occupied by ions, (based upon ionic radii), the mean bond coordination, and the deviation of bond coordination are descriptors that correlate with the room-temperature coefficient of thermal expansion for these materials found in widely accessible databases. Correlation is greatly improved by combining these descriptors in a multi-dimensional fit. This fit reinforces the physical interpretation that open space combined with low mean coordination and a variety of local bond coordinations leads to materials with lower coefficients of thermal expansion, materials with single-valued local coordination and less open space have the highest coefficients of thermal expansion.

I. INTRODUCTION

Because of the potential for temperature gradients or other thermal stresses to cause electronic devices to fail, knowledge of the coefficients of thermal expansion (CTE) of materials is important. Either active materials with desired thermal properties or composites of active and compensating materials can mitigate the ill effects of thermal expansion in real devices^{1,2}. A compensating material must be chemically and electrically compatible with the functional material and will typically contract with increasing temperature; i.e. it will exhibit negative thermal expansion (NTE). While the CTEs for many materials have been cataloged, the set of known NTE materials is small, and materials appropriate for specific applications may not yet be available. A means of rapidly predicting the thermal expansion properties of yet-to-be investigated materials will be extremely useful.

The displacement of the equilibrium positions of atoms in a material with temperature is the source of thermal expansion. While anharmonicity in the vibrations of bonded pairs of atoms will drive the atoms farther apart with increasing temperature, crystal structure also plays an essential role in the specific thermal expansion characteristics of a material, providing behaviors over the range from positive thermal expansion (PTE) to NTE. Accurate theoretical modeling of thermal expansion in materials necessitates quantum mechanical calculations and dynamical calculations or, minimally, quasi-harmonic modeling. As a result, typical calculations of thermal expansion address the microscopic causes of experimentally-observed CTE on a case-by-case basis. Especially prevalent recently are experimental and theoretical investigations of materials that exhibit NTE, such as ZrW_2O_8 ³⁻¹⁵, M_2O (with $M = \text{Cu, Ag, Au}$)¹⁶, ReO_3 ^{17,18}, and ScF_3 .^{19,20} Except for materials with very similar electronic and structural properties, a global picture capable of guiding searches for new materials with desired thermal expansion characteristics is slow

to emerge. While a useful high-throughput approach to estimating material thermal properties, employing fits of DFT-calculated energy-volume curves to equations of state and employing a quasi-harmonic Debye approximation, has been developed²¹ and recently improved²², the approach we present provides an complementary picture through its focus on local structural properties. Comprehensive reviews of thermal expansion in materials, emphasizing NTE in both theory and experiment, can be found in Refs. 23 and 24.

For microscopic atomic displacements to create NTE, the motions of the atoms must carry them into spaces already existing within the lattice, while simultaneously drawing neighboring ions closer together. It is well-known^{23,24} that the definition of the volumetric thermal expansion α_v ,

$$\alpha_v = \frac{1}{V} \left(\frac{\partial V}{\partial T} \right)_P, \quad (1)$$

can, with the help of a Maxwell relation, be rewritten as

$$\alpha_v = -\frac{1}{V} \left(\frac{\partial S}{\partial P} \right)_T, \quad (2)$$

which shows that for a material to exhibit NTE, entropy must increase with pressure, contrary to typical expectations. Typically, decreasing the volume available to a free particle is associated with decreasing entropy. The definition in Eq. 2 is isothermal, which effectively means that the momentum space contribution to entropy changes negligibly relative to the real space contribution. From this we deduce that applying pressure in an NTE material effectively increases the volume available to its constituent atoms. On the other hand, applying pressure to PTE materials (at constant temperature) results in decreasing entropy, implying a corresponding decrease in the effective volume available to the atoms that follows from the same line of argument used above. In order for there to be more volume available to the atoms within

a crystalline material despite decreasing total volume, atomic motions must be directed more significantly into the open spaces within the lattice. In other words, the atomic motions possess significant components in directions perpendicular to the bonds with nearest-neighbor atoms. The difference between NTE and PTE is therefore directly related to the degree to which ionic thermal displacements are longitudinal or transverse with respect to the bonds. Experimental evidence supporting this view is found, for example, in a study of NTE in ScF_3 , in which inelastic neutron scattering shows that the Sc-F bonds lengthen with increasing temperature and that the material contracts over a wide temperature range as a result of large transverse motions of the F ions¹⁹. In our recent molecular dynamics investigation, we demonstrated that thermal expansion in a single structure, with expanding bonds modeled with first- and second-neighbor interactions via Morse potentials, can be varied from NTE to PTE by increasing the second-neighbor interaction strength relative to the first-neighbor interactions.²⁵ By adjusting second-neighbor interactions, we reduced the transverse motions of the light ions, resulting in the emergence of PTE in the model. The key element permitting transverse motion in these examples is low bond coordination, which is necessarily linked to open lattices.

We propose that an approach to predicting thermal expansion can be found by scanning the literature for the structures of crystals, focusing on quantities that may have a relationship to the entropy of the material and its potential to increase or decrease with respect to pressure, such as the space occupied by ions and their bonding coordinations. We employ the wealth of structural information in databases such as the Inorganic Crystal Structure Database (ICSD)^{26,27} and the Crystallographic Open Database (COD)^{28–32} in this work. By correlating materials with known CTE to their structures, we can begin to determine useful descriptors for thermal expansion. As a result of the lack of complete temperature dependences of the CTE for many of the materials investigated here, we focus on structures stable at room temperature and their CTEs. In Section II, we discuss the physical underpinnings for the quantities that we propose for descriptors of CTE. In Section III, we present the choice of descriptors from the original list of quantities of interest along with the result of performing a fit using the descriptors developed. We conclude with a discussion of the implications this correlation will have in the search for materials with desired thermal expansion properties.

II. PROPOSED DESCRIPTORS

For each atom in a unit cell of each material, the number of nearest neighbors and formal oxidation state are determined. From this information we obtain ionic radii³³ r_i for each ion and an estimate of the volume each ion occupies (assuming it occupies a sphere of vol-

ume $V_i = \frac{4}{3}\pi r_i^3$). The fractional volume occupied is the total volume estimated for all the atoms in the unit cell divided by the volume of the unit cell $V_{\text{u.c.}}$:

$$v = \frac{1}{V_{\text{u.c.}}} \sum_i V_i. \quad (3)$$

A complete list of the data used for this investigation is provided in the Appendix. As seen in Fig. 1, thermal expansion data for the materials we sampled show that there is a relationship between thermal expansion and the volume occupied by atoms in the lattice; more open space corresponds to a greater likelihood for NTE.

The cluster of points with $\alpha_v \gtrsim 90 \times 10^{-6}/\text{K}$ in Fig. 1 consists of binary materials that have the rock salt structure, with the corresponding high coordination providing an explanation for the large positive thermal expansion in these materials. We note that Coulomb interactions between second neighbors will be repulsive and strong. The data point with the highest volume occupied and very low PTE belongs to cubic BN. Because of its zincblende structure, the B and N atoms in BN have tetrahedral coordination. We also note that BN has a high bulk modulus, which implies that the tetrahedral bonds are strong and maintain their directionality. Although the volume occupancy of BN is high, the strong bonds produce a smaller thermal expansion. (The situation in BN is reminiscent of the diamond phases of C, Si, and Ge, which all have small values of α_v at room temperature. It is notable that Si exhibits NTE at lower temperatures, indicating a lower barrier to transverse motions of its atoms.) Although low bond coordination in a material is a possible descriptor to predict thermal expansion coefficients, it is not sufficient on its own. Low coordination, such as seen in BN, is a result of directional bonding. But low coordination also occurs at the linking atoms in a crystal structure that is composed of groups of atoms forming stable units, as is the case for ScF_3 , ReO_3 and other perovskite materials. Collective rotational-vibrational motion of these units is known as a rigid unit mode (RUM)³⁴. RUMs are cited as the underlying cause of NTE in ScF_3 , ReO_3 ¹⁸, and, arguably, in ZrW_2O_8 ¹². The atoms at the linking points of the rigid units typically are two-fold coordinated, while the atoms at the centers are more highly coordinated. The thermal vibrations of the RUM tend to be low frequency, carrying low-coordination atoms significant distances in directions transverse to the bonds. We note that the RUM is also presented as a foundational model for displacive phase transitions³⁵ connecting these vibrational modes to symmetry changes at phase boundaries. The importance of phase boundaries for which the higher-temperature phase has a smaller volume (and higher entropy) has been introduced as a thermodynamic cause of NTE^{36,37}. As the temperature is increased toward the phase boundary from below, thermal fluctuations introducing an increasing fraction of the lower-volume, higher-entropy structure into the lattice is shown to be the necessary condition for NTE^{36,37}. This is consistent with the observation above

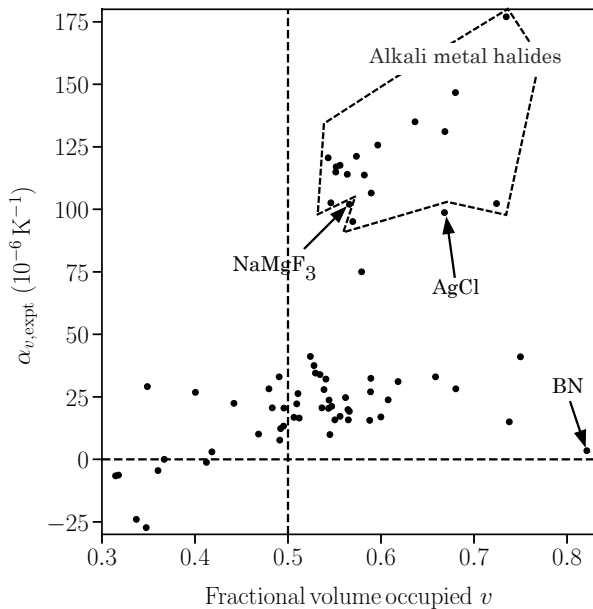


FIG. 1. The experimental coefficient of thermal expansion ($\alpha_{v,\text{expt}}$) is plotted as a function of fractional volume occupied as defined in Eq. 3 for the materials gleaned from the literature. Apparently, NTE is possible only when v is less than ≈ 0.5 .

that greater entropy must be associated with smaller volume in NTE materials. As a result of these observations, we suggest that the variability of bonding coordinations in a material, indicative of rigid units, is a key structural quantity to be used as a descriptor for thermal expansion.

III. RESULTS AND DISCUSSION

Quantities extracted in the search for descriptors, in addition to v , are the mean bond coordination $\langle c \rangle$, its standard deviation σ_c , the mean atomic mass $\langle m \rangle$, the minimum mass m_{\min} , the maximum mass m_{\max} , and the standard deviation of mass σ_m . In Fig. 2, we display the linear correlations between descriptor candidates and the experimental α_v . In addition, we include unitless ratios $\sigma_c/\langle c \rangle$, $\sigma_m/\langle m \rangle$, and the ratio of minimum to maximum mass m_{\min}/m_{\max} . The quantities that have the strongest correlations with the α_v are v and $\langle c \rangle$, with correlations 0.48 and 0.55, respectively. The next-most-highly correlated quantity is σ_c , with a (negative) correlation of -0.42 to α_v . Furthermore, this quantity does not correlate with either the volume ratio v or the mean coordination $\langle c \rangle$. The candidates involving mass have low correlations with α_v and are neglected. Finally, we determine that v , σ_c , and $\langle c \rangle$ are a good set of descriptors.

To discover the relationships between these descrip-

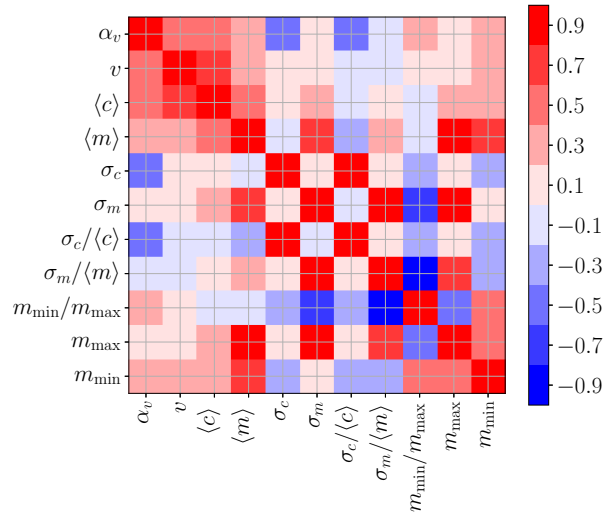


FIG. 2. (Color online) The correlations (Pearson- r) between candidate descriptors and the coefficient of thermal expansion α_v for 71 materials taken from the literature. Moderate linear correlation with α_v is found for both the mean coordination and occupied volume. Weak-to-moderate correlation is exhibited by both the mean mass and the ratio of minimum to maximum atomic mass. Focusing on quantities which correlate strongly with α_v leads to a set of three descriptors: the occupied volume, the mean coordination, and standard deviation of the coordination.

tors and the experimentally-measured values of α_v , we performed a second-order polynomial fit of these three descriptors to the 71 materials in our data sample, using the relation

$$\alpha_{v,\text{calc}}(v, \langle c \rangle, \sigma_c) = \sum_{i+j+k \leq 2} c_{ijk} v^i \langle c \rangle^j (\sigma_c)^k. \quad (4)$$

The correlation plot for this fit is displayed in Fig. 3, and the coefficients are listed in Table I. The correlation coefficient is 0.83, and the RMS-deviation between the fit and the data is $26 \times 10^{-6} \text{ K}^{-1}$, a noticeable improvement in correlation over the data displayed in Fig. 1, with outlying (alkali-halide) points more closely fit. Including only linear terms in the fit did not produce an acceptable interpolation. Adding cubic terms produced a substantially better fit but the trends we describe below are unchanged by the additional terms. Points to the right of the diagonal are ones for which the model predicts thermal expansion greater than the experimentally measured value. The previously noted deviation in BN has been nearly eliminated. The predicted values for the ionic solids have also been increased toward their experimental values. The material with largest positive deviation ($\alpha_{v,\text{calc}} > \alpha_{v,\text{expt}}$) is Bi_2Se_3 . The largest negative deviation arises for LiI .

In order to visualize the model and to isolate ranges of the descriptors that characterize the CTE, we present

TABLE I. The parameters used in Eq. 4 to evaluate $\alpha_{v,\text{calc}}(v, \langle c \rangle, \sigma_c)$. Uncertainties are based on a nominal experimental α_v error of 10^{-6} K^{-1} .

i	j	k	c_{ijk}
0	0	0	-290 ± 5
1	0	0	685 ± 9
0	1	0	15 ± 1
0	0	1	103.7 ± 0.8
1	1	0	123 ± 1
1	0	1	-132 ± 1
0	1	1	-14.3 ± 0.1
2	0	0	-964 ± 7
0	2	0	-5.7 ± 0.2
0	0	2	12.0 ± 0.1

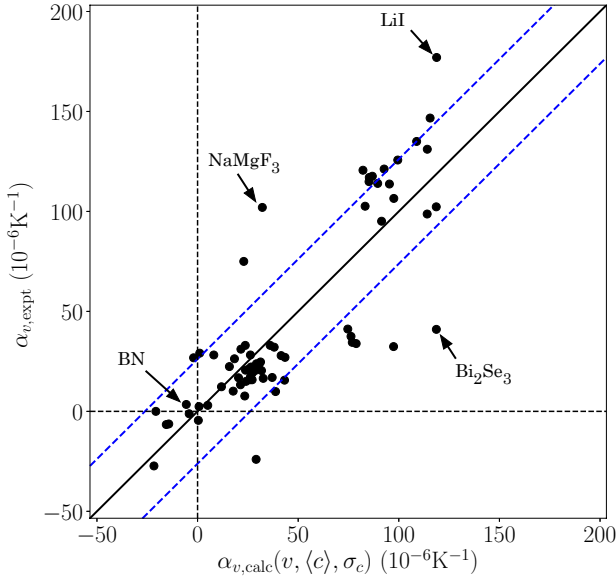


FIG. 3. (Color online) Correlation plot of room-temperature experimental and calculated α_v generated by a ten-parameter second-order polynomial fit to experimental data using Eq. 4 with the parameters in Table I. The root-mean-squared deviation of the calculated coefficients of expansion, indicated with blue dashed lines, is $26 \times 10^{-6} \text{ K}^{-1}$. The Pearson- r for this fit is 0.83.

contours of constant $\alpha_{v,\text{calc}}$ across the ranges of $\langle c \rangle$ and σ_c at fixed volume ratios $v = 0.3, 0.4, \dots, 0.8$ in Fig. 4. Superimposed on the contours are points indicating the descriptor values of data used in the fit, including volume ratios within ± 0.05 of the value of v displayed in the corresponding panel. NTE materials are indicated in Fig. 4 with red dots. As noted previously, materials with the lowest filled volume ratios are most likely to have NTE. In panels (a) and (b) in Fig. 4 we see that the NTE materials generally have $\langle c \rangle \lesssim 4$ and coordination devi-

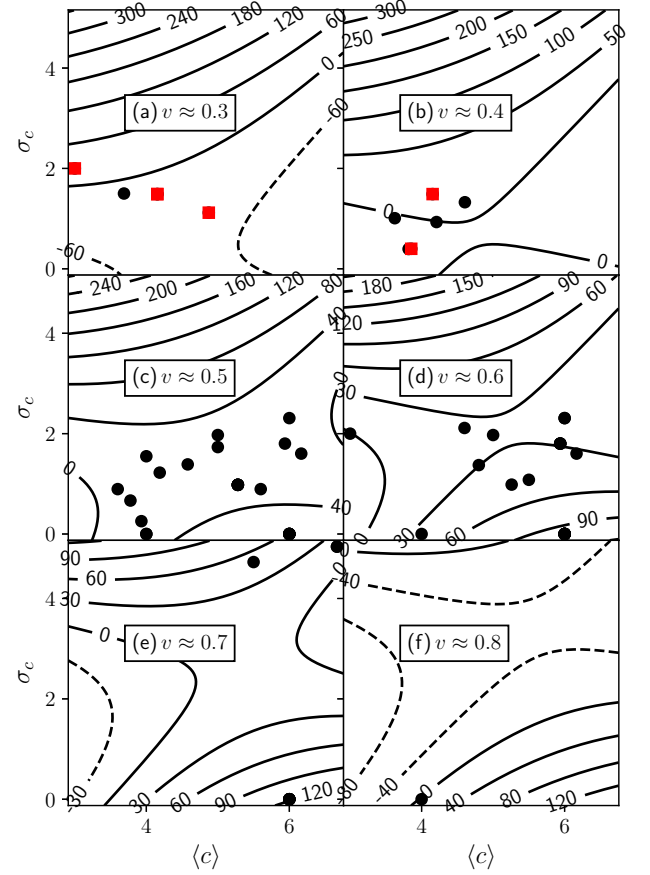


FIG. 4. (Color online) Contour plots showing the dependence of the calculated α_v upon $\langle c \rangle$ and σ_c at fixed volume ratios v , as indicated. The markers plotted display the descriptor values for the materials used in the fit, with black circles for PTE materials and red squares for NTE materials. The volume ratios for the data points displayed in each panel fall within ± 0.05 of the value of v indicated in each panel. All experimental α_v values are measured at room temperature.

ations $\sigma_c \approx 2$, the exception being LiAlSiO_4 , which has $\alpha_{v,\text{expt}} = 1.2 \times 10^{-6} \text{ K}^{-1}$. In addition to open space, important contributors to NTE are low mean coordination and a distribution of local coordinations.

The majority of materials in this work have volume ratios around 0.5 to 0.6 and are displayed in panels (c) and (d) in Fig. 4. These materials also generally possess $\alpha_{v,\text{expt}} \approx 30 \times 10^{-6} \text{ K}^{-1}$ that would be considered typical. Mean coordinations are generally greater than that found in the NTE materials in panels (a) and (b). Many of the materials in this volume ratio neighborhood have zero coordination variance as a result of their simple structures. In particular, the ions in the rock-salt-structured alkali halides have identical coordination en-

TABLE II – Continued

Material	COD	ICSD	$\alpha_{v,\text{expt}}$	$\alpha_{v,\text{calc}}$	v	$\langle c \rangle$	σ_c
Al ₂ Si ₅ O	1011204		13.29 ⁴⁰	21.33	0.50	4.19	1.22
Al ₂ W ₃ O ₁₂		90936	−4.50 ⁴²	0.38	0.36	4.15	1.49
BN	9008834		3.45 ⁴¹	−5.60	0.82	4.00	0.00
BPO ₄	1010299		28.20 ⁴³	8.06	0.48	3.60	0.89
BeAl ₂ O ₄	9000120		23.80 ⁴⁰	29.25	0.61	4.80	1.37
BeO		15620	16.95 ⁴¹	37.08	0.60	4.00	0.00
Be ₂ SiO ₄	9001088		16.80 ⁴⁰	20.35	0.51	3.93	0.26
Be ₃ Al ₂ Si ₆ O ₁₈	1010541		3.00 ⁴⁴	5.06	0.42	4.21	0.93
Bi ₂ Se ₃	1530736		41.01 ⁴⁵	118.67	0.75	6.00	0.00
CaGeO ₃	9000904		31.10 ⁴⁰	21.53	0.62	6.00	2.31
CaOTi ₃	1000022		75.00 ⁴⁴	22.95	0.58	6.00	2.31
CaO	1000044		37.50 ³⁹	76.25	0.53	6.00	0.00
Ca ₃ Al ₂ Si ₃ O ₁₂	9000236		19.20 ⁴⁶	27.21	0.57	5.94	1.80
Ca ₃ Fe ₂ Si ₃ O ₁₂	9007693		20.60 ⁴⁰	23.82	0.54	5.94	1.80
Cr ₂ FeO ₄	9007325		9.90 ⁴⁰	38.76	0.55	5.28	0.98
Cr ₂ MgO ₄	9006180		16.50 ⁴⁰	32.62	0.51	5.28	0.98
FeO	1011169		33.90 ⁴⁰	78.82	0.53	6.00	0.00
FeTiO ₃	1011033		27.90 ⁴⁰	41.52	0.54	5.60	0.89
Fe ₃ O ₄	9002316		20.60 ⁴⁰	25.50	0.48	5.28	0.98
GaN	1010168		10.11 ⁴⁷	17.70	0.47	4.00	0.00
GeZn ₂ O ₄		16173	0.00 ⁴⁸	−20.73	0.37	3.82	0.39
HfO ₂	1528988		15.80 ⁴⁰	26.12	0.55	6.17	1.60
KBr	9008650		117.60 ⁴⁹	86.85	0.56	6.00	0.00
KCl		165593	114.90 ³⁹	85.20	0.55	6.00	0.00
KF	9008652		95.10 ⁵⁰	91.44	0.57	6.00	0.00
KI	9008654		113.70 ⁵¹	95.34	0.58	6.00	0.00
KNbO ₃	1531431		15.00 ⁴⁴	24.05	0.74	5.50	4.73
LiAlSiO ₄	9002541		−1.20 ⁴⁰	−4.16	0.41	3.85	0.40
LiAlSi ₂ O ₆	9000347		22.20 ⁴⁰	26.62	0.51	4.58	1.39
LiBr	9008664		146.70 ⁵⁰	115.56	0.68	6.00	0.00
LiCl	9008665		131.10 ⁵⁰	114.16	0.67	6.00	0.00
LiF		181799	106.50 ⁵²	97.51	0.59	6.00	0.00
LiI	9008669		177.00 ³⁹	118.79	0.73	6.00	0.00
MgF ₂	1526229		33.00 ⁴⁴	23.71	0.49	4.00	1.55
MgFe ₂ O ₄	1011245		20.50 ⁴⁰	28.78	0.50	5.28	0.98
MgGeO ₃	9000957		22.40 ⁴⁰	15.82	0.44	4.61	1.33
MgO		9863	32.40 ⁵³	97.40	0.59	6.00	0.00
Mg ₂ GeO ₄	9010486		32.10 ⁴⁰	38.08	0.54	5.28	0.98
MnO	1010393		34.50 ⁴⁰	76.88	0.53	6.00	0.00
Mo ₃ Fe ₂ O ₁₂	1524203		29.10 ⁵⁴	1.06	0.35	3.69	1.50
NaAlSi ₂ O ₆	9000143		24.70 ⁴⁰	31.29	0.56	5.00	1.97
NaAlSi ₃ O ₈	9000526		26.80 ⁴⁰	−1.99	0.40	3.62	1.01
NaBr	9007464		125.70 ⁵⁰	99.48	0.60	6.00	0.00
NaCl	4320809		121.20 ⁵⁵	92.71	0.57	6.00	0.00
NaCrSi ₂ O ₆	1531195		20.40 ⁴⁰	31.77	0.54	5.00	1.97
NaF		262837	102.60 ⁴⁹	83.26	0.55	6.00	0.00
NaI	9008681		135.00 ⁵⁰	108.86	0.64	6.00	0.00
NaMgF ₃	9001612		102.00 ⁴⁴	32.18	0.57	4.60	2.11
NaNbO ₃	1011064		33.00 ⁴⁴	36.08	0.66	6.67	5.03
ReO ₃		77679	2.4 ¹⁸	0.73	0.60	3.00	2.00
RbBr	9008706		117.00 ⁴⁹	85.33	0.55	6.00	0.00
RbCl		22166	120.60 ⁵⁶	82.19	0.54	6.00	0.00
RbI	9008710		114.00 ⁵¹	89.51	0.56	6.00	0.00
ScAlO ₃	9005883		27.00 ⁴⁰	43.45	0.59	5.50	1.08
ScF ₃		261072	−24.00 ⁵⁷	29.10	0.34	3.00	2.00
Sc ₂ Mo ₃ O ₁₂		391467	−6.30 ⁵⁸	−14.32	0.32	4.15	1.49
Continued...							

TABLE II – Continued

Material	COD	ICSD	$\alpha_{v,\text{expt}}$	$\alpha_{v,\text{calc}}$	v	$\langle c \rangle$	σ_c
Sc ₂ W ₃ O ₁₂		50941	−6.60 ⁵⁸	−15.54	0.31	4.15	1.49
SrO		163625	41.16 ³⁹	74.65	0.52	6.00	0.00
SrTiO ₃	7212245		28.20 ⁵⁹	26.26	0.68	6.67	5.03
SrZrO ₃	1521387		26.30 ⁵⁹	18.34	0.51	6.00	2.31
TiO ₂	4102355		23.70 ⁴⁴	30.64	0.54	5.00	1.73
ZrO ₂	2300544		21.20 ⁴⁰	25.53	0.55	6.17	1.60
ZrSiO ₄	1011265		12.30 ⁴⁰	11.87	0.49	3.78	0.67
ZrW ₂ O ₈		262061	−27.30 ⁶⁰	−21.68	0.35	4.87	1.12

ACKNOWLEDGMENTS

This work has been supported by the Department of Energy Office of Basic Energy Sciences, under grant num-

ber DE-FG02-07ER46431. A.M.R. acknowledges support from the Office of Naval Research under grant number N00014-17-1-2574. Computational support was provided by the National Energy Research Scientific Computing Center (NERSC).

- * joseph.schick@villanova.edu
- ¹ C. Lind, *Materials* **5**, 1125 (2012).
 - ² J. Chen, L. Hu, J. Deng, and X. Xing, *Chem. Soc. Rev.* **44**, 3522 (2015).
 - ³ T. A. Mary, J. S. O. Evans, T. Vogt, and A. W. Sleight, *Science* **272**, 90 (1996), <http://www.sciencemag.org/content/272/5258/90.full.pdf>.
 - ⁴ A. K. A. Pryde, K. D. Hammonds, M. T. Dove, V. Heine, J. D. Gale, and M. C. Warren, *J. Phys.: Condens. Matter* **8**, 10973 (1996).
 - ⁵ A. P. Ramirez and G. R. Kowach, *Phys. Rev. Lett.* **80**, 4903 (1998).
 - ⁶ G. Ernst, C. Broholm, G. R. Kowach, and A. P. Ramirez, *Nature* **396**, 147 (1998).
 - ⁷ R. Mittal and S. L. Chaplot, *Phys. Rev. B* **60**, 7234 (1999).
 - ⁸ R. Mittal, S. L. Chaplot, H. Schober, and T. A. Mary, *Phys. Rev. Lett.* **86**, 4692 (2001).
 - ⁹ D. Cao, F. Bridges, G. R. Kowach, and A. P. Ramirez, *Phys. Rev. Lett.* **89**, 215902 (2002).
 - ¹⁰ D. Cao, F. Bridges, G. R. Kowach, and A. P. Ramirez, *Phys. Rev. B* **68**, 014303 (2003).
 - ¹¹ J. N. Hancock, C. Turpen, Z. Schlesinger, G. R. Kowach, and A. P. Ramirez, *Phys. Rev. Lett.* **93**, 225501 (2004).
 - ¹² M. G. Tucker, A. L. Goodwin, M. T. Dove, D. A. Keen, S. A. Wells, and J. S. O. Evans, *Phys. Rev. Lett.* **95**, 255501 (2005).
 - ¹³ V. Gava, A. L. Martinotto, and C. A. Perottoni, *Phys. Rev. Lett.* **109**, 195503 (2012).
 - ¹⁴ F. Bridges, T. Keiber, P. Juhas, S. J. L. Billinge, L. Sutton, J. Wilde, and G. R. Kowach, *Phys. Rev. Lett.* **112**, 045505 (2014).
 - ¹⁵ A. Sanson, *Chemistry of Materials* **26**, 3716 (2014), <http://dx.doi.org/10.1021/cm501107w>.
 - ¹⁶ M. K. Gupta, R. Mittal, S. L. Chaplot, and S. Rols, *Journal of Applied Physics* **115**, 093507 (2014).
 - ¹⁷ E. S. Božin, T. Chatterji, and S. J. L. Billinge, *Phys. Rev. B* **86**, 094110 (2012).
 - ¹⁸ T. Chatterji, T. C. Hansen, M. Brunelli, and P. F. Henry, *Appl. Phys. Lett.* **94**, 241902 (2009).
 - ¹⁹ C. W. Li, X. Tang, J. A. Muñoz, J. B. Keith, S. J. Tracy, D. L. Abernathy, and B. Fultz, *Phys. Rev. Lett.* **107**, 195504 (2011).
 - ²⁰ P. Lazar, T. Bučko, and J. Hafner, *Phys. Rev. B* **92**, 224302 (2015).
 - ²¹ C. Toher, J. J. Plata, O. Levy, M. de Jong, M. Asta, M. B. Nardelli, and S. Curtarolo, *Phys. Rev. B* **90**, 174107 (2014).
 - ²² C. Toher, C. Oses, J. J. Plata, D. Hicks, F. Rose, O. Levy, M. de Jong, M. Asta, M. Fornari, M. Buongiorno Nardelli, and S. Curtarolo, *Phys. Rev. Materials* **1**, 015401 (2017).
 - ²³ G. D. Barrera, J. A. O. Bruno, T. H. K. Barron, and N. L. Allan, *Journal of Physics: Condensed Matter* **17**, R217 (2005).
 - ²⁴ M. T. Dove and H. Fang, *Reports on Progress in Physics* **79**, 066503 (2016).
 - ²⁵ J. T. Schick and A. M. Rappe, *Phys. Rev. B* **93**, 214304 (2016).
 - ²⁶ G. Bergerhoff, *Crystallographic Databases*, edited by F. H. Allan, G. Bergerhoff, and R. Sievers (International Union of Crystallography, 1987).
 - ²⁷ A. Belsky, M. Hellenbrandt, V. L. Karen, and P. Luksch, *Acta Crystallographica Section B* **58**, 364 (2002).
 - ²⁸ A. Merkys, A. Vaitkus, J. Butkus, M. Okulič-Kazarinas, V. Kairys, and S. Gražulis, *Journal of Applied Crystallography* **49**, 292 (2016).
 - ²⁹ S. Gražulis, A. Merkys, A. Vaitkus, and M. Okulič-Kazarinas, *Journal of Applied Crystallography* **48**, 85 (2015).
 - ³⁰ S. Gražulis, A. Daškevič, A. Merkys, D. Chateigner, L. Lutterotti, M. Quiros, N. R. Serebryanaya, P. Moeck, R. T. Downs, and A. Le Bail, *Nucleic Acids Research* **40**, D420 (2012).
 - ³¹ S. Gražulis, D. Chateigner, R. T. Downs, A. F. T. Yokochi, M. Quiros, L. Lutterotti, E. Manakova, J. Butkus, P. Moeck, and A. Le Bail, *Journal of Applied Crystallography* **42**, 726 (2009).
 - ³² R. T. Downs and M. Hall-Wallace, *American Mineralogist* **88**, 247 (2003).

- ³³ R. D. Shannon, *Acta Crystallographica Section A* **32**, 751 (1976).
- ³⁴ K. D. Hammonds, M. T. Dove, A. P. Giddy, V. Heine, and B. Winkler, *American Mineralogist* **81**, 1057 (1996).
- ³⁵ M. T. Dove, *American Mineralogist* **82**, 213 (1997).
- ³⁶ Z.-K. Liu, Y. Wang, and S.-L. Shang, *Scripta Materialia* **65**, 664 (2011).
- ³⁷ Z.-K. Liu, Y. Wang, and S. Shang, *Scientific Reports* **4**, 7043 (2014).
- ³⁸ P. W. Sparks and C. A. Swenson, *Phys. Rev.* **163**, 779 (1967).
- ³⁹ S. Kumar, *Proceedings of the National Institute of Sciences of India: Physical Sciences* **25**, 364 (1959).
- ⁴⁰ Y. Fei, "Mineral physics & crystallography: A handbook of physical constants," (American Geophysical Union, 1995) Chap. 2-4.
- ⁴¹ G. A. Slack and S. F. Bartram, *Journal of Applied Physics* **46**, 89 (1975).
- ⁴² D. A. Woodcock, P. Lightfoot, L. A. Villaescusa, M.-J. Díaz-Cabañas, M. A. Camblor, and D. Engberg, *Chemistry of Materials* **11**, 2508 (1999).
- ⁴³ S. Achary and A. Tyagi, *Journal of Solid State Chemistry* **177**, 3918 (2004).
- ⁴⁴ H. D. Megaw, *Materials Research Bulletin* **6**, 1007 (1971).
- ⁴⁵ X. Chen, H. D. Zhou, A. Kiswandhi, I. Miotkowski, Y. P. Chen, P. A. Sharma, A. L. Lima Sharma, M. A. Hekmaty, D. Smirnov, and Z. Jiang, *Applied Physics Letters* **99**, 261912 (2011).
- ⁴⁶ D. G. Isaak, O. L. Anderson, and H. Oda, *Physics and Chemistry of Minerals* **19**, 106 (1992).
- ⁴⁷ H. Iwanaga, A. Kunishige, and S. Takeuchi, *Journal of Materials Science* **35**, 2451 (2000).
- ⁴⁸ R. Stevens, B. F. Woodfield, J. Boerio-Goates, and M. K. Crawford, *The Journal of Chemical Thermodynamics* **36**, 349 (2004).
- ⁴⁹ P. Pathak, J. Trivedi, and N. Vasavada, *Acta Crystallographica Section A* **29**, 477 (1973), cited By.
- ⁵⁰ J. E. Rapp and H. D. Merchant, *Journal of Applied Physics* **44**, 3919 (1973).
- ⁵¹ P. Pathak and N. Pandya, *Acta Crystallographica Section A* **31**, 155 (1975), cited By.
- ⁵² P. Pathak and N. Vasavada, *Acta Crystallographica Section A* **28**, 30 (1972), cited By.
- ⁵³ I. Suzuki, *Journal of Physics of the Earth* **23**, 145 (1975).
- ⁵⁴ A. Tyagi, S. Achary, and M. Mathews, *Journal of Alloys and Compounds* **339**, 207 (2002).
- ⁵⁵ P. Pathak and N. Vasavada, *Acta Crystallographica Section A* **26**, 655 (1970), cited By.
- ⁵⁶ K. Srivastava and H. Merchant, *Journal of Physics and Chemistry of Solids* **34**, 2069 (1973).
- ⁵⁷ B. K. Greve, K. L. Martin, P. L. Lee, P. J. Chupas, K. W. Chapman, and A. P. Wilkinson, *Journal of the American Chemical Society* **132**, 15496 (2010).
- ⁵⁸ J. Evans, T. Mary, and A. Sleight, *Journal of Solid State Chemistry* **133**, 580 (1997).
- ⁵⁹ D. de Ligny and P. Richet, *Phys. Rev. B* **53**, 3013 (1996).
- ⁶⁰ J. S. O. Evans, T. A. Mary, T. Vogt, M. A. Subramanian, and A. W. Sleight, *Chemistry of Materials* **8**, 2809 (1996), <http://dx.doi.org/10.1021/cm9602959>.